High Bandwidth Planar Power Divider

by

Md Ayatullah Maktoomi

Under the Supervision of Dr. Mohammad S. Hashmi

Indraprastha Institute of Information Technology Delhi

June, 2016

High Bandwidth Planar Power Divider

by

Md Ayatullah Maktoomi

Submitted

in partial fulfillment of the requirements for the degree of

Master of Technology in
Electronics and Communication Engineering

to the

Indraprastha Institute of Information Technology Delhi

June, 2016

Certificate

This is to certify that the thesis titled "*High Bandwidth Planar Power Divider*" being submitted by Md Ayatullah Maktoomi to the Indraprastha Institute of Information Technology Delhi, for the award of the degree of Master of Technology, is an original work carried out by him under my supervision. In my opinion, the thesis has reached the standards fulfilling the requirements of the regulations relating to the degree. The results contained in this thesis have not been submitted in part or full to any other university or institute for the award of any degree/diploma.

June, 2016
Dr. Mohammad S. Hashmi

Department of Electronics & Communication Engineering
Indraprastha Institute of Information Technology Delhi
New Delhi 110 020

Abstract

The power dividers are one of the most ubiquitous passive circuit elements in RF/Microwave applications. They are widely used in antenna arrays, balanced amplifiers, mixers, frequency multipliers etc. as power combiners or splitters. The Wilkinson power divider (WPD) and the Gysel power divider (GPD) are the two most useful of all the power dividers because of it low insertion loss, matched ports and isolated outputs ports. The conventional WPD has a simple structure and good performance except that its bandwidth, especially the isolation bandwidth, is limited. Therefore, this thesis aimed at exploring the ways to enhance this Figure of Merit (FOM). To that end, a combination of the GPD and WPD architectures with a single isolation resistor is proposed as one of the methods to achieve higher isolation bandwidth. Simulation results indicate that for 15dB reference, a return loss bandwidth of 72% is possible as compared to 36% for the conventional methods. Furthermore, a WPD utilizing the concept of port extension is also proposed that provides complete DC isolation along with a higher bandwidth. This technique is fully planar and does not require any extra lumped element in the isolation network to achieve a measured isolation bandwidth of 62%.

Relevant Publications

1. M. A. Maktoomi and M. S. Hashmi, "A novel power divider structure using the gysel and wilkinson power dividers with only one grounded resistor," 2015 *IEEE MTT-S International Microwave and RF Conference (IMaRC)*, Hyderabad, pp. 227-229, 2015.
2. M. A. Maktoomi, M. S. Hashmi and F. M. Ghannouchi, “Theory and design of a novel wide-band dc isolated Wilkinson power divider,” *IEEE Microw. Wireless Compon. Lett*., 2016 (Accepted, available online at IEEExplore).

Acknowledgements

This thesis would not have been possible without huge support from my supervisor, family, friends, and colleagues. I wish to express my special gratitude to my research advisor Dr. Mohammad S Hashmi, Assistant Professor, IIIT Delhi, for giving me the chance to work under his supervision. I am very grateful for his continuous support and encouragements in the course of this work. I would like to sincerely thank Dr. Fadhel M Ghannouchi for supporting my stay at the iRadio Lab, University of Calgary, Canada. My thanks also go to my family members, friends and colleagues.

Contents

Chapter 1

Power Divider/Splitter: Introduction

Power dividers (splitters)/combiners are one of the most basic components required in high-frequency applications. They are widely used in various microwave devices and systems, such as antennas, power amplifiers, linearization of power amplifiers, test setups, and measurement circuits, etc [1].

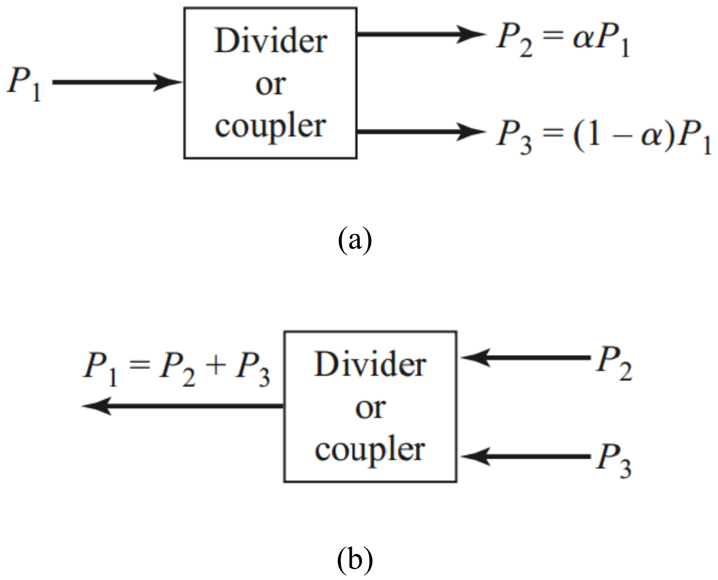

Fig. 1.1. Power (a) splitting and (b) combining [1].

Black box diagrams of power splitters and combiners are depicted in Fig. 1.1. In power division or splitting, an input signal is divided into two (or more) output signals of lesser power. α denotes the power division ratio and the power division operation may not be always equal (α = 0.5) and the operation may be lossy as in a resistive power divider. In contrast, a power combiner accepts two or more input signals and combines them at an output port. Power combining and splitting devices are usually thought as three-port networks take the form of T-junctions and other power dividers. However, four-port networks such as directional couplers are very commonly used for this purpose as well. Power dividers usually provide in-phase output signals with an equal power division ratio (3 dB), but unequal power division ratios are also possible. A key difference between coupler and power divider is that coupler creates a phase shift between the output signals. In most circumstances, power dividers provide zero phase shift; couplers come with 90º or 180º phase shifts [2]. However, arbitrary phase shift couplers are also possible.

Since, majority of the power dividers and combiners are reciprocal devices, the same device can be used for combining and splitting. Therefore, henceforth, only the term power divider will be used to mean both a combining as well as a splitting device.

The lossless power divider, the resistive power divider, and the Wilkinson power divider are three main types of planar power dividers. As will be explained later, a Gysel power divider can be thought as variant of the Wilkinson power divider.

1.1 Lossless Power Divider

The T-junction power divider is shown in Fig. 1.2. Considering that transmission line losses are absent, this power divider is lossless. It can be proved that a 3-port network

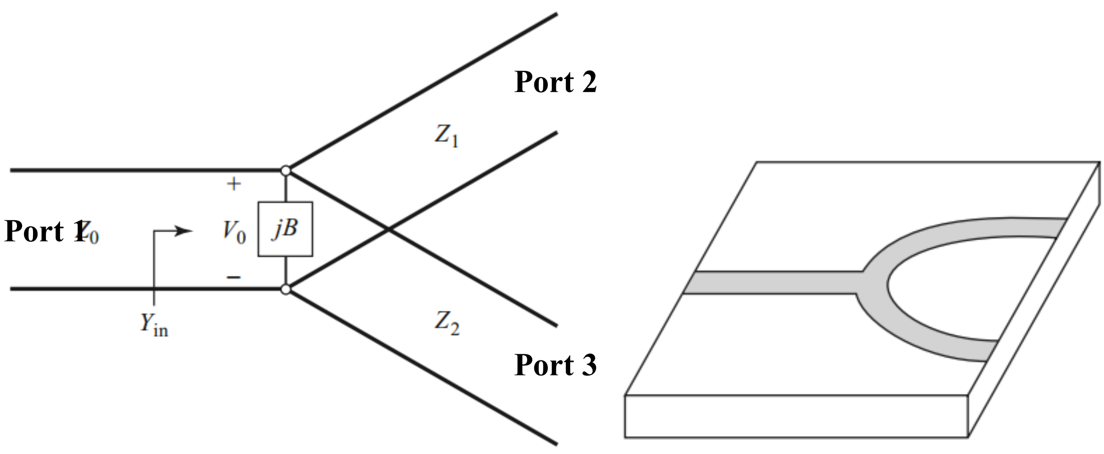

Fig. 1.2. (a) A lossless power divider and (b) its microstrip implementation [1].

cannot be lossless, reciprocal, and matched at all ports at the same time [1]. For a physically realizable 3-port device, any one of these three conditions is relaxed. And, therefore, the (ideal) junction shown in Fig. 1.2 cannot be matched at three ports simultaneously. The susceptance jB at the junction represents the junction discontinuity effect. If B is negligible or is compensated somehow, then for matching to exist at the port 1:

$$\frac{1}{Z_0} = \frac{1}{Z_1} + \frac{1}{Z_2} \tag{1.1}$$

The output line impedances Z_1 and Z_2 can be selected to get various power division ratios. In general, if powers at port 2 and at port 3 are to be divided such that $P_2 = \alpha P_{in}$ and $P_3 = (1-\alpha) P_{in}$, then the following relation holds in Fig. 1.2(a):

$$P_{in} = \frac{1}{2}\frac{V_0^2}{Z_0} \tag{1.2}$$

$$P_2 = \frac{1}{2}\frac{V_0^2}{Z_1} = \alpha P_{in} \tag{1.3}$$

$$P_3 = \frac{1}{2}\frac{V_0^2}{Z_2} = (1-\alpha) P_{in} \tag{1.4}$$

Simplifying (1.2) to (1.4):

$$Z_1 = \frac{Z_0}{\alpha} \tag{1.5}$$

$$Z_2 = \frac{Z_0}{1-\alpha} \tag{1.6}$$

The input impedance at port 1, Z_{in}, is given by:

$$Z_{in} = Z_1 \,||\, Z_2 = Z_0 \tag{1.7}$$

Therefore, the input port is matched. However, looking from port 1 and port 2, the input impedances are not equal to Z_0, therefore not all the ports are matched. Moreover, isolation of this divider depends on the power division ratio, and in general, it is poor.

1.2 Resistive Power Divider

A resistive power divider is shown in Fig. 1.3. It basically comprises of 3 resistors arranged as a wye-network; a delta configuration is also possible. Since this power divider contains lossy elements, it can be made simultaneously matched at all the three ports.

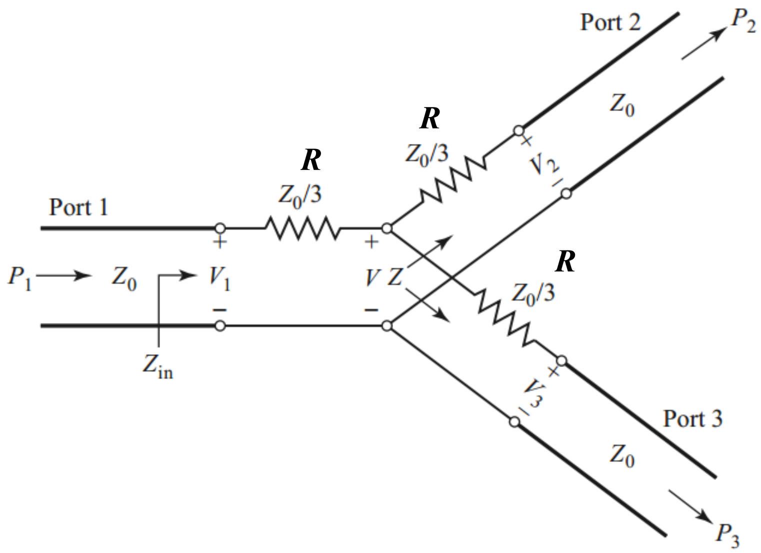

Fig. 1.3. A resistive equal power divider [1].

The required values of resistors, R, could be derived as follows. In Fig. 1.3, Z is the input impedance looking into the resistor R followed by port termination impedance, Z_0. Thus,

$$Z = R + Z_0 \tag{1.8}$$

$$Z_{in} = R + Z/2 = Z_0 \tag{1.9}$$

Simplifying (1.8) and (1.9),

$$R = Z_0/3 \tag{1.10}$$

Because the network is symmetric, output ports are also matched with the above value of R, that is, $S_{11} = S_{22} = S_{33} = 0$.

If V_1 is the input voltage, the voltage at the junction, V, can be found using voltage divider theorem as follows:

$$V = \frac{Z/2}{Z_0/3 + Z/2} V_1 = \frac{2}{3} V_1 \tag{1.11}$$

and then, voltages V_2 and V_3 at the output ports can be expressed as follows:

$$V_2 = V_3 = \frac{Z_0}{Z_0 + Z_0/3} V = \frac{3}{4} V = \frac{1}{2} V_1 \tag{1.12}$$

And, therefore, $S_{21} = S_{31} = S_{23} = 1/2$, that is, output power is 6dB below the input power. Resistive power divider is a lossy power divider. Also, the isolation is only 6dB.

1.3 The Wilkinson Power Divider

A Wilkinson power divider (WPD) is a lossy three-port network having all ports matched, with good isolation between output ports. Schematic of an equal split two-way WPD is depicted in Fig. 1.4. It comprises of two quarter wavelength transmission lines each having a characteristic impedance of $\sqrt{2}Z_0$ and an isolation resistor $R = 2Z_0$.

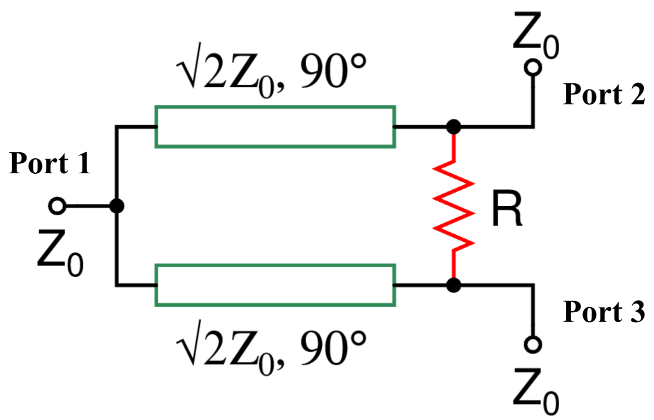

Fig. 1.4. An equal amplitude, two-way Wilkinson power divider (WPD).

When a signal enters into port 1, it splits into equal-amplitude, equal-phase output signals at ports 2 and 3. Because of symmetry, each end of the isolation resistor is at the same potential, no current flows through it and therefore the resistor is decoupled from the input. Thus, the operation boils down to matching $2Z_0$ to Z_0, as the two branches are, in effect, in parallel. The quarter wavelength transmission lines are to facilitate this impedance transformation and the characteristic impedance of the quarter wavelength lines must be equal to $1.414Z_0$. When a signal enters into port 2, a part of it goes clockwise through the resistor and part goes counterclockwise through the upper arm, then splits at the input port, then continues counterclockwise through the lower arm toward port 3. The recombining signals at port 3 end up equal in amplitude and they are 180 degrees out of phase due to the half-wavelength that the CCW signal travels. The two signal voltages subtract to zero at port 3 and the signal disappears, at least under ideal circumstances. In real couplers, there is a finite phase through the resistor that will limit the isolation of the output ports [3].

The WPD can be readily analyzed using even-odd mode procedure [1]. To that end, the WPD shown earlier in Fig. 1.4 is redrawn in Fig. 1.5 in symmetric and normalized form. In the normalized form each impedance is divided by the port impedance, Z_0.

Now in the even-mode, $V_{g2}=V_{g3}=2V_0$ and therefore, each point along the middle horizontal symmetric line is open-circuited. On the other hand, in the odd-mode, $V_{g2}=-V_{g3}=2V_0$ and therefore, each point along the axis of symmetry is short-circuited.

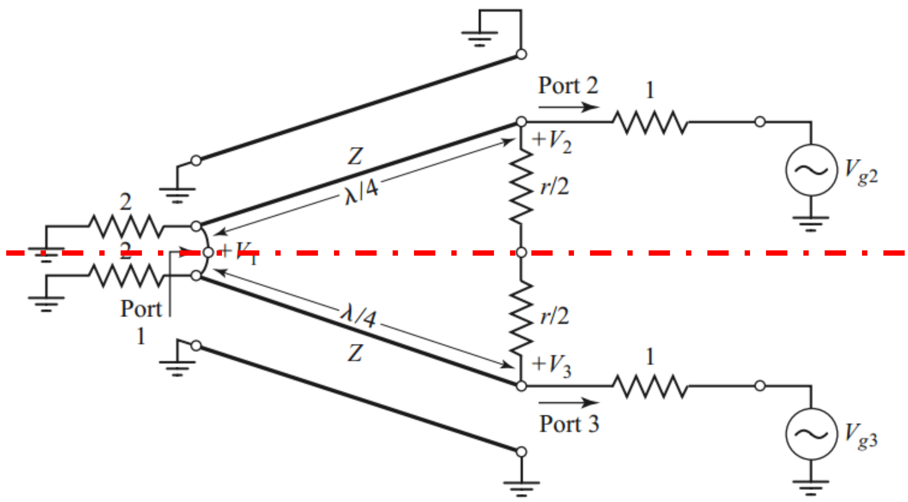

Fig. 1.5. The symmetric and normalized form of the WPD [1].

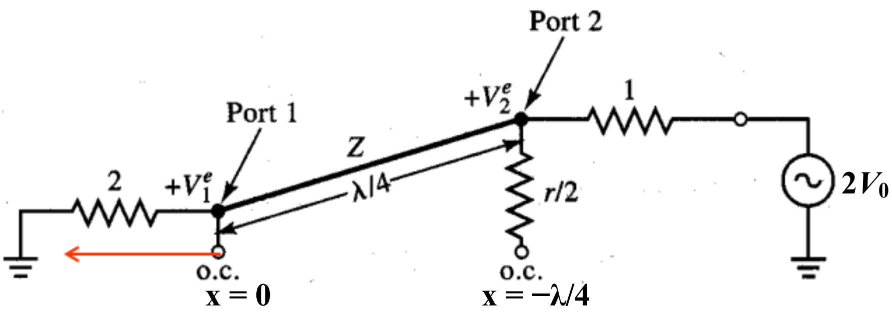

Fig. 1.6. The even-mode equivalent network of the WPD.

The even-mode half circuit is shown in Fig. 1.6. It is apparent that the isolation resistor has no role in this mode as the one of its end is open-circuited. Therefore, the input impedance at port 2 in this mode is given by:

$$Z_{in}^{e} = \frac{Z^2}{2} \tag{1.13}$$

Since, for matching, $Z_{in}^{e} = 1$ and, thus Z=√2. Moreover, $V_2^e = V_0$, using the voltage divider theorem. Now assuming the x-axis as depicted in Fig. 1.6, the voltage on the transmission line can be expressed as follows:

$$V(x) = V^{+}(e^{-j\beta x} + \Gamma e^{j\beta x}) \tag{1.14}$$

$$V_2^e = jV^{+}(1-\Gamma) = V_0 \tag{1.15}$$

Which gives,

$$V_1^e = V^{+}(1+\Gamma) = jV_0 \frac{\Gamma+1}{\Gamma-1} \tag{1.16}$$

Since, $\Gamma = \dfrac{2-\sqrt{2}}{2+\sqrt{2}}$, therefore,

$$V_1^e = -j\sqrt{2}V_0 \tag{1.17}$$

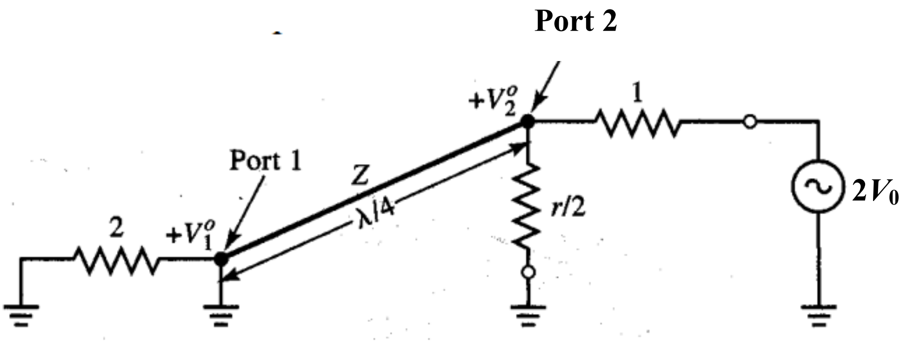

Fig. 1.7. The odd-mode equivalent network of the WPD.

For odd-mode excitation, the half circuit is depicted in Fig. 1.7. Since, port 1 is short-circuited and the line is λ/4 long, the input impedance looking into the line at port 2 is infinite. And therefore, for matching at port 2; $r = 2$. Then, $V_1^o = 0$ and $V_2^o = V_0$.

Finally, as pointed out earlier, the equivalent circuit looking from the port 1 consists of two quarter wavelength lines in parallel loaded with a unity resistor (since the isolation resistor has no impact due to zero voltage across its ends), the normalized input impedance is just unity. It can be concluded from the above analysis that $S_{11} = S_{22} = S_{33} = S_{23} = S_{32} = 0$, $S_{12} = S_{21} = S_{13} = S_{31} = -j/\sqrt{2}$. The ideal line performance of the WPD is shown in Fig. 1.8. Due to the use of quarter wavelength lines, the response is narrow-band.

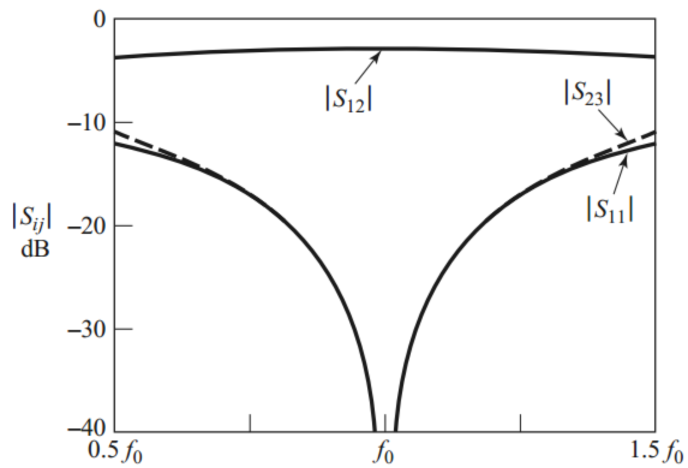

Fig. 1.8. Simulated frequency response of 3dB WPD [1].

1.4 The Gysel Power Divider

As shown in Fig. 1.9, a Gysel power divider (GPD) is also a three port device like a WPD, but it has two isolation resistors whose other ends are connected to ground [3]. The major advantage of the GPD is its much better heat dissipation capabilities. If we consider the WPD shown earlier in Fig. 1.4, there is no connection to the ground, the resistor lies on the top plane. In contrast, in a GPD the two resistors need to be connected to the ground plane and that makes the way for proper heat dissipation.

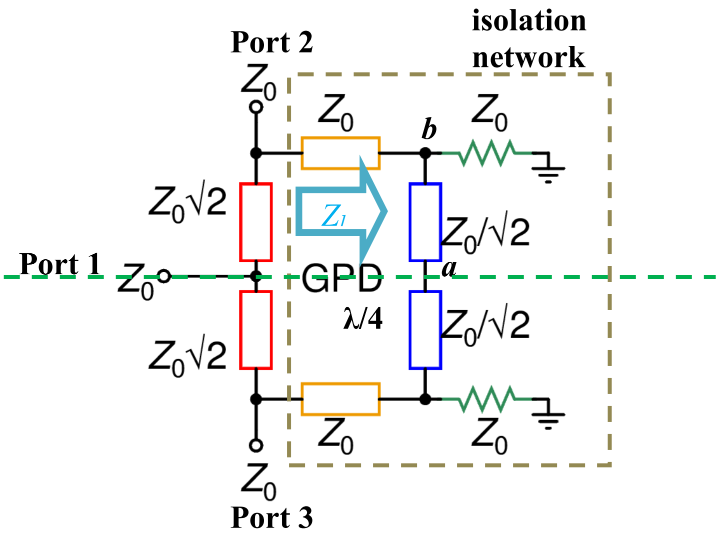

Fig. 1.9. An equal amplitude, two-way Gysel power divider (GPD).

A one to one comparison between Figs. 1.4 and 1.9 reveals that the single floating isolation resistor found in the WPD is replaced by an isolation network consisting of transmission lines and grounded resistors as depicted using a dashed box in Fig. 1.9. It is apparent that the GPD is also a symmetrical structure; even-odd-mode analysis can be used to analyze this network. However, since, the WPD has already been analyzed in the previous section, suffice is to show that GPD is similar to the WPD. Specifically, it is to be shown that the part of GPD inside the box is equivalent to isolation resistor of WPD during even-odd-mode analysis. To that end, two intermediate nodes have been designated as '*a*' and '*b*' and an axis of symmetry has been shown as well. During the even mode analysis, each point on the axis of symmetry is open-circuited, while during odd-mode each point is short-circuited.

Now, during even-mode, point *a* is open-circuited that causes a short circuit to appear at point *b* due to the vertical quarter wave line (blue). That, in turn, forces an open circuit to get transferred from point *b* to the port 2, that is Z_l is infinitely large. This is exactly what happens in a WPD, and therefore, equivalence of WPD and GPD is evident during the even-mode operation.

During odd mode, a short-circuit appears at the node *a*, causing an open circuit to appear at node *b*. Due to quarter-wave line (yellow), the isolation resistor of Z_0 is transformed into $Z_l = Z_0^2 / Z_0 = Z_0$. Again, this is exactly what port 2 and 3 see towards resistor in a WPD. Thus, the equivalence between WPD and GPD is also evident during the odd-mode operation.

As a final point, since the equivalence between a simple isolation resistor of WPD to that of the boxed isolation network of GPD exists only at a single frequency, therefore, the bandwidth performance of GPD is inferior to that of the WPD.

1.5 Literature Overview

It is apparent from Fig. 1.8 that the required matching occurs only at a single frequency in the WPD and it is the utilization of quarter wavelength lines as transformers which causes narrow band performance. Moreover, since equivalence of the isolation resistor in the WPD to that of the isolation network in the GPD also exists only at a single frequency; the performance of the GPD is also narrowband. Although, the heat-dissipation is better in the GPD, the bandwidth performance is inferior to the WPD.

The current state-of-the-art research in power dividers, in general, and in WPD/GPD, in particular, has focused in many directions. Primarily, the focus is on realizing multi-band capabilities [4-11], wideband design [12-19], miniaturization [20-23] and achieving additional filtering [24] and harmonic suppression [20]. For example, A multi-section approach for the WPD as depicted in Fig. 1.10 was introduced by Cohn [12]. It was shown that the divider's bandwidth increases with its number of sections; 2.5:1 for two sections; 4:1 for three sections; 5.5:1 for four sections; and 10:1 for seven section. It is a good technique but size is larger and more lumped resistors are required. A similar technique employing multiple coupled line sections was reported in [13].

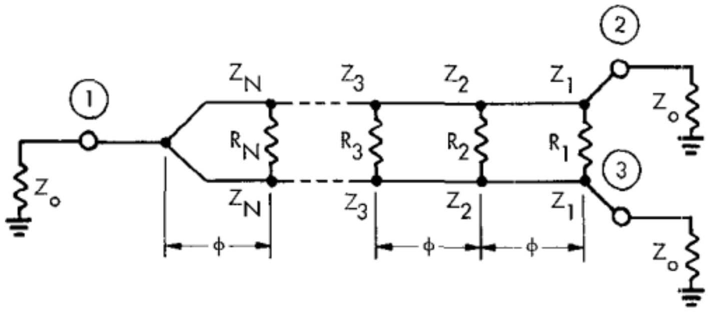

Fig. 1.10. Multi-section WPD [12]

A numerical algorithm based on the method of least squares (MLS) was reported for the design and optimization of a WPD [15]. As shown in Fig. 1.11, this design is asymmetric. The advantage of this method is arbitrary power division between its outputs in a specified frequency bandwidth.

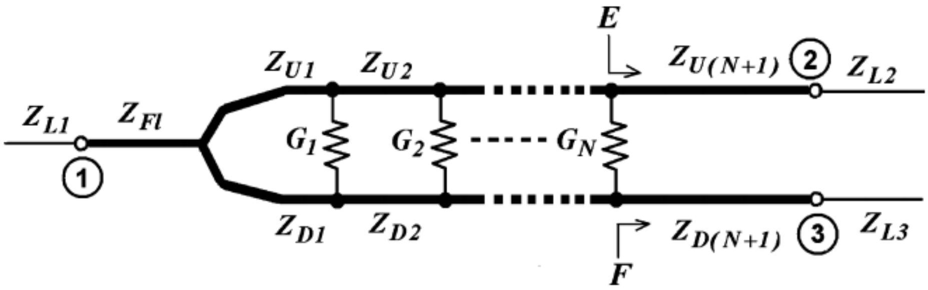

Fig. 1.11 N-section Wilkinson power divider [15].

Utilization of impedance transformation using tapered lines has been reported for wide operation bandwidth [17]. A pair of quarter wavelength short-circuited stubs and/or parallel coupled lines to two symmetrical output ports can be used for good performance in terms of equal power splitting over the ultra-wideband range [18]. Yet another, and currently a prevalent technique is to use complex isolation networks [25]. In fact, the literature on power divider is vast and it is not possible to mention all of them here; many other relevant works have been referred in the respective chapters.

1.6 Statement of the Problem

Widening of bandwidth of power divider has always been given huge attention by the research community. In this regard, much of prior art either uses multi-section/ tapered lines or has tried to modify the isolation network itself to achieve wideband performance.

Therefore, in this thesis, two not so common techniques have been investigated. The first one combines the GPD and WPD schemes to achieve both a wider bandwidth as well as good heat-dissipation capabilities. In fact, the proposed technique utilizes only one resistor as compared to two in the conventional GPD. Considering 15dB return-loss reference, the bandwidth is 72% for the proposed design whereas it is only 36% for earlier reported design.

The second design makes use of port-matching technique to achieve a better performance without modifying the isolation network. In addition, due to the use of parallel coupled lines, an inherent DC-block functionality is achieved. Specifically, the measured isolation bandwidth is 62% considering 15dB reference.

1.7 Thesis Outline

A brief discussion of various conventional power dividers and literature review was presented in the current chapter. Afterwards, Chapter 2 presents analysis, design and simulation of a combined GPD and WPD structure. A clear strategy to design this power divider has been illustrated through a flowchart. Reviews of some of the relevant previous works have also been included.

Chapter 3 discusses the analysis and design of wideband WPD utilizing the concept of port matching. Specifically, a parallel coupled line has been used to provide impedance matching at each port of a WPD core structure. Various case studies with regard to possible matching scenario arising from the availability of independent variables have been studied. This chapter also shows a prototype and measurement results that compare well with the EM simulated results. Finally, conclusion and references are included at the end.

Chapter 2

Power Divider using GPD and WPD

2.1 Introduction

A power divider is a very important passive building block in RF/Microwave components and systems. They are routinely used in balanced amplifiers, mixers, antenna arrays etc [26-27]. The Wilkinson power divider (WPD) and the Gysel power divider (GPD) are the two most widely used divider types. Although, a WPD has good bandwidth but due to the presence of a floating resistor, the heat dissipation is poor. In contrast, since the grounded resistors are present in GPD; its heat handling capability is better. However, the bandwidth of GPD is inferior to that of a WPD [28].

One of the recent research focuses in the GPD design is to reduce the number of isolation resistors, from the usual two to unity [26, 29]. The technique reported in [26] is limited by the fact that, in general, the coupled line in microstrip needs compensation [30]. In the GPD reported in [29], the conventional π-length transmission line (TL) is replaced by a parallel combination of a T-type network and another π-length TL, but at the expense of reduced bandwidth [29]. Efforts are also directed towards the bandwidth enhancement of the GPD [28], [15] and in multi-band design [31]. The technique used in [15] needs optimization whereas the one reported in [28], again, needs two isolation resistors.

In this chapter, a novel divider structure is proposed, which uses only one isolation resistor, yet has more bandwidth than the conventional GPD [32].

2.2 Proposed Divider: Analysis and Design

In this section, design equations of conventional divider are summarized. Subsequently, the proposed divider is analyzed to obtain closed-form design equations.

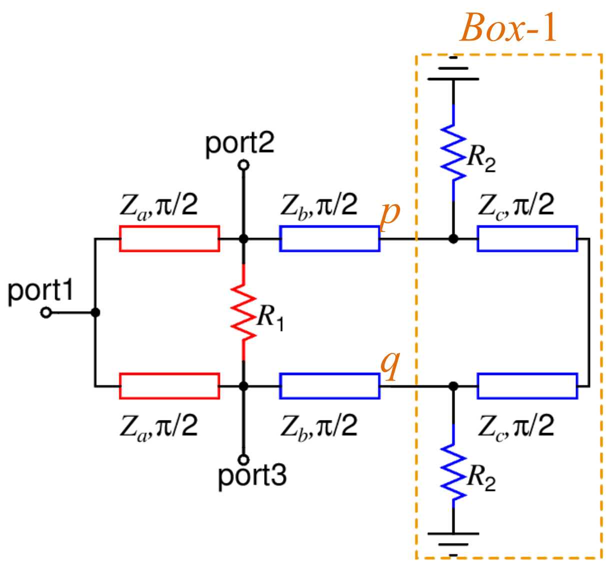

Fig. 2.1. Conventional combined WPD and GPD with two grounded resistors [28].

2.2.1 Review of the Conventional Design

The conventional design as reported in [28] is shown in Fig. 2.1. The floating resistor, R_1 comes from the WPD and the two grounded resistors, R_2 are contributed by the GPD part. The electrical lengths of all the TL sections are 90º at the design frequency. The design equations for the conventional divider are summarized as follows:

$$Z_a = \sqrt{2}Z_0 \text{ and } Z_b = R_2 \tag{2.1}$$

$$R_1 = \frac{2R_2Z_0}{R_2 - Z_0} \tag{2.2}$$

Z_c influences only the bandwidth; it is usually equal to $Z_0/\sqrt{2}$ to achieve a wider bandwidth and port termination $Z_0 = 50\Omega$.

2.2.2 Proposed Design

The proposed divider is shown in Fig. 2.2. It is apparent that it has only one grounded resistor. The two 90º TL sections with characteristic impedance Z_C in the conventional divider is now replaced with two TL sections of different characteristic impedance, namely, Z_{C1} and Z_{C2}.

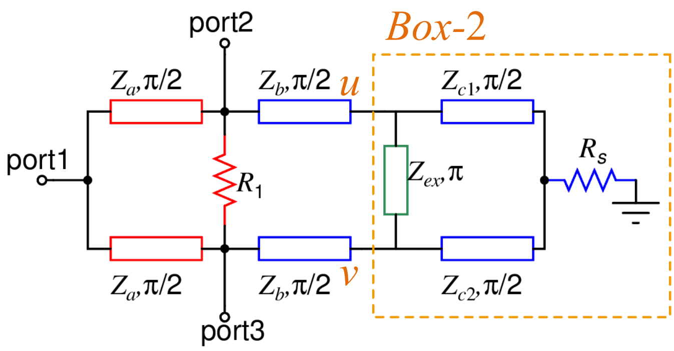

Fig. 2.2 Proposed combined WPD and GPD with only one grounded resistors [32].

Since, the only difference between the conventional and the proposed divider is in the structures within the dashed boxes, derivation of the design equations of the proposed divider can be easily done by equating the ABCD parameters of Box1 (*p*-*q*) and Box2 (*u*-*v*).

The ABCD parameter of Box1 is as follows:

$$[ABCD]_{p-q} = [ABCD]_{R_2} \times [ABCD]_{Z_C} \times [ABCD]_{R_2}$$

$$= \begin{bmatrix} 1 & 0 \\ G_2 & 1 \end{bmatrix} \begin{bmatrix} -1 & 0 \\ 0 & -1 \end{bmatrix} \begin{bmatrix} 1 & 0 \\ G_2 & 1 \end{bmatrix}$$

$$= \begin{bmatrix} -1 & 0 \\ -2G_2 & -1 \end{bmatrix} \tag{2.3}$$

Where, $G_2 = 1/R_2$.

Now, the ABCD parameter of the Box2 can be found by using the following ABCD parameter of the T-network (Z_{C1}-R_S-Z_{C2}) and that of the 180º TL with characteristic impedance Z_{ex}.

$$[ABCD]_{Z_{C1}-R_S-Z_{C2}} = \begin{bmatrix} 0 & jZ_{C1} \\ \dfrac{j}{Z_{C1}} & 0 \end{bmatrix} \begin{bmatrix} 1 & 0 \\ G_S & 1 \end{bmatrix} \begin{bmatrix} 0 & jZ_{C2} \\ \dfrac{j}{Z_{C2}} & 0 \end{bmatrix} \tag{2.4}$$

$$[ABCD]_{Z_{ex},180^{\circ}} = \begin{bmatrix} -1 & 0 \\ 0 & -1 \end{bmatrix} \quad (2.5)$$

Where, $G_S = 1/R_S$.

And, therefore,

$$[ABCD]_{u-v} = \begin{bmatrix} -1 & 0 \\ \dfrac{\left(1-\dfrac{Z_{C2}}{Z_{C1}}\right)\left(\dfrac{Z_{C1}}{Z_{C2}}-1\right)}{-G_S Z_{C1} Z_{C2}} & -1 \end{bmatrix} \quad (2.6)$$

Equating the R.H.S of (2.3) that to the R.H.S of (2.6), results into following equation:

$$\frac{\left(1-\dfrac{Z_{C2}}{Z_{C1}}\right)\left(\dfrac{Z_{C1}}{Z_{C2}}-1\right)}{-G_S Z_{C1} Z_{C2}} = -2G_2 \quad (2.7)$$

And, therefore,

$$Z_{C1} = \left|\frac{1-x}{x}\right|\sqrt{\frac{1}{2G_2 G_S}} \quad (2.8)$$

$$Z_{C2} = xZ_{C1} \quad (2.9)$$

where x is an independently chosen constant such that the impedances Z_{C1} and Z_{C2} are physically realizable in microstrip technology, that is, they are within the range 20Ω to 150Ω.

2.3 Design Steps

The design procedure of the proposed divider based on the equations derived in the previous sections is depicted in the flowchart of Fig. 2.3. The value of R_2 has trade-off with the heat-handling capability. Its higher value implies lesser current, and thus, lesser amount of heat flowing to ground plane. Furthermore, x is an independent variable in the designer's hand; it must be selected carefully so that the resulting structure is physically realizable. The constant x can lie anywhere between, $2/15 \leq x \leq 15/2$.

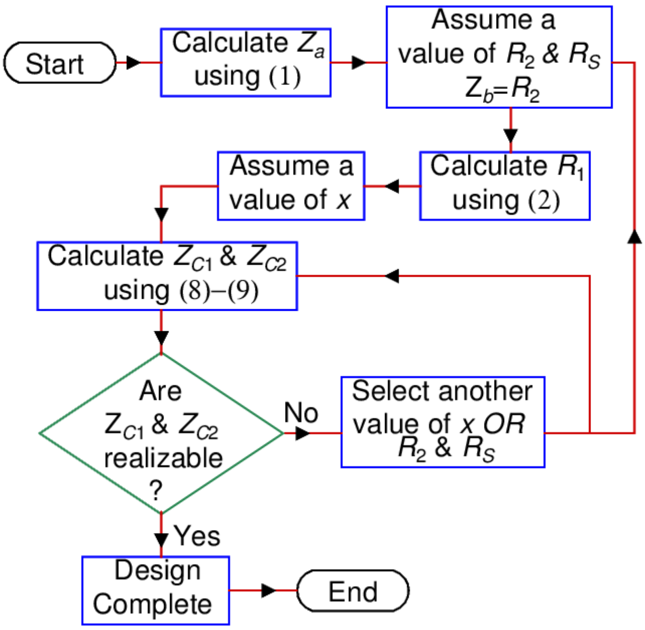

Fig. 2.3. Flowchart showing the steps involved in design of proposed divider. Equation number (1) depicted in this flowchart refers to equation (2.1) in this chapter, and so on.

2.4 Simulation and Comparison

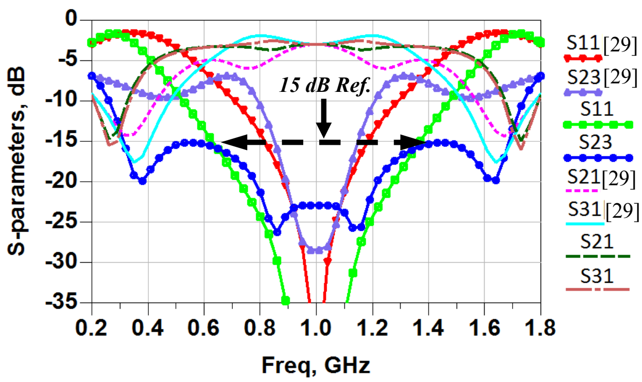

Fig. 2.4. Simulated S-parameters of proposed divider. Simulated S-parameters of [29] is also depicted in this figure for a comparison.

Using the design procedure outlined in the previous section, one possible design parameters of the proposed design is as follows: Z_a=70.7Ω, Z_b=100Ω, Z_{ex}=35.35Ω, Z_{C1}=100Ω, Z_{C2}=33.33Ω, and R_S=100Ω. The simulated results of the proposed design are depicted in Fig. 2.4 along with the simulated results of [29]. A higher bandwidth as compared to the conventional design is evident from the plots. For example, the 15dB return loss bandwidth is 72% for the proposed design whereas it is only 36% in case of [29]. It is also apparent that the transmission parameters are smoother for the proposed design.

It is pointed out in the interest of audience that in [29], simplification leading to (6) from its previous step should result into the following equation (rather than that with a minus sign):

$$\frac{p}{q}+\frac{q}{p}=2pq+2 \tag{2.10}$$

This mistake also leads to some further mistakes in calculations discussed in Section III of [29]. Therefore, while simulating the design of [29], values obtained using (2.10) have been used.

A comparison with state-of-the-art designs are given in Table 2.1. It is apparent that the proposed design with 72% bandwidth (BW) has acceptable isolation of 23dB while utilizing only one grounded resistor.

TABLE 2.1 COMPARISION WITH STATE-OF-ART DESIGNS

Ref.	Parameters		
	No of Grounded Resistors	***BW (%)***	***Isolation (dB)***
[26]	2[a]	65[a]	36
[28]	2	66	50
[29]	1	36	28
This Work	1	72	23

[a]For equal power division

The isolation in case of [28] seems pretty good at the center frequency, but it is instructive to compare the same with the proposed design. To that end, design of [28] is simulated and corresponding isolation is shown in Fig. 2.5 along with that of the proposed design. It is pretty clear that while the isolation of the proposed design is within acceptable limits, at the same time the 15dB isolation BW is higher for the proposed design by 200MHz.

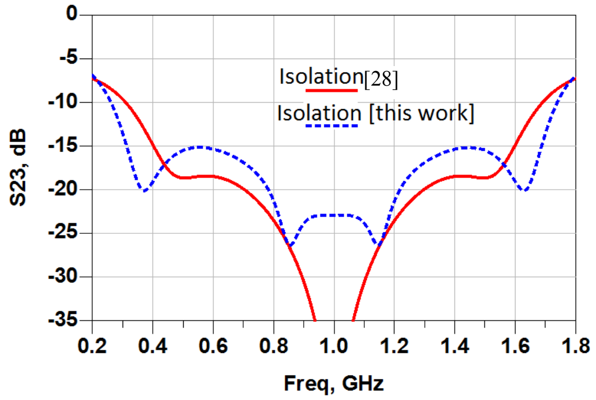

Fig. 2.5. Simulated isolation of proposed divider *vs.* that of the [28]

2.5 Conclusion

A novel technique to design a power divider by combining the WPD and GPD have been discussed in this chapter. The idea has been to take bandwidth advantage of the WPD whereas exploiting the heat-handling capability of GPD. A unique contribution of this work while doing so has been to reduce the number of grounded isolation resistor to unity. In this effort, while the isolation gets deteriorated at the central frequency, but still well within the acceptable limits, the overall isolation bandwidth is also found to be enhanced. A limitation when compared to the conventional GPD and WPD is the area overhead, but this is ubiquitous trade-off scenario commonly found in engineering design.

Chapter 3

A Novel WPD with High Isolation Bandwidth

3.1 Introduction

Power dividers are extremely important components in RF/microwave industrial applications [33-34]. The conventional Wilkinson power divider (WPD) has low isolation bandwidth; consequently, many interesting solutions have been reported to extend its bandwidth [35]. Recently, a design utilizing microstrip-to- stripline transition has also been reported, but it requires processing on bottom plane as well [36]. Perhaps, the most popular and current approach to enhance bandwidth is the modification of isolation network of the conventional WPD [25, 35]. However, increased number of lumped components increases their design complexity [37].

In this chapter, a novel WPD design is presented that utilizes port matching using coupled lines to enhance the isolation bandwidth of the conventional WPD without modifying the isolation network [40]. Inherently present DC isolation of the proposed WPD makes it a very suitable candidate in balanced amplifier designs as it does away with the requirement of coupling capacitors.

3.2 The Proposed WPD

The schematic of the proposed equal-split WPD is shown in Fig. 3.1. It comprises of a WPD-core, and three coupled lines at each port for matching. Z_{el} (Z_{er}), Z_{ol} (Z_{or}), and θ_l (θ_r) represents the even- and odd-mode characteristic impedances and the electrical length of the coupled line(s) on the left (right). Z_m and θ_m are the characteristic impedance and the electrical length of the transmission-lines of WPD-core. R is the isolation resistor, whereas Z_s denotes the port terminations. Each electrical length is equal to 90° at the design frequency, f_0. Y_l (Y_r) is the input admittance looking into the left (right) coupled line (s) which is (are) terminated into Z_s. $Y_{eq,in}$ and $Y_{eq,out}$ are the equivalent input and output admittances of the WPD-core.

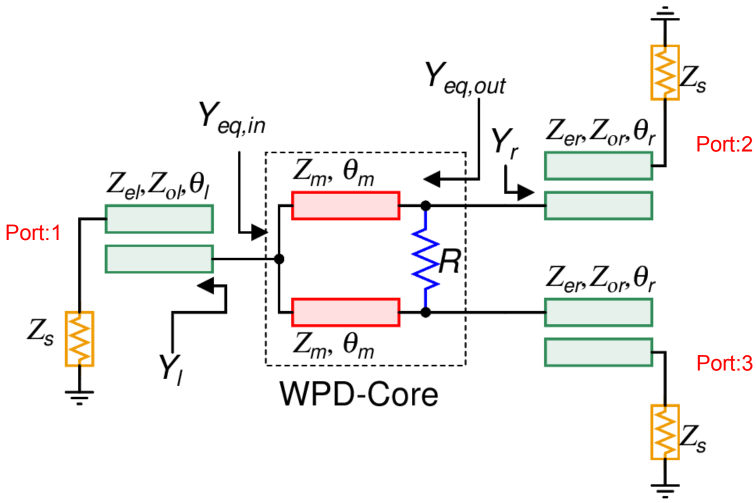

Fig. 3.1. Proposed wideband Wilkinson power divider (WPD). Coupled lines at each port serve as matching network.

3.2.1 Design Equations of the proposed WPD

The equivalent admittance of the WPD-core at f_0, that is, when θ_m=90º, are given as follows [38]:

$$Y_{eq,in}\Big|_{f_0} = \frac{R}{Z_m^2} \tag{3.1}$$

$$Y_{eq,out}\Big|_{f_0} = \frac{2}{R} \tag{3.2}$$

Similarly, the equivalent admittance of the coupled line at f_0 can be deduced by substituting $\theta_2 = 90$º in equations (9a)-(9b) in [30], and they are as follows:

$$Y_l\Big|_{f_0} = \frac{4Z_s}{\left(Z_{el} - Z_{ol}\right)^2} \tag{3.3}$$

$$Y_r\Big|_{f_0} = \frac{4Z_s}{\left(Z_{er} - Z_{or}\right)^2} \tag{3.4}$$

Now, for matching condition, one needs to set $Y_{eq,in}\Big|_{f_0} = \left(Y_l\Big|_{f_0}\right)^*$ and, $Y_{eq,out}\Big|_{f_0} = \left(Y_r\Big|_{f_0}\right)^*$, which yields the following design equations:

$$Z_{el} - Z_{ol} = 2Z_m\sqrt{Z_s / R} \tag{3.5}$$

$$Z_{er} - Z_{or} = \sqrt{2Z_s R} \quad . \tag{3.6}$$

(3.5)-(3.6) are general design equations of the proposed WPD.

Substituting *R* from (3.6) into (3.5), yields the following design constraint:

$$Z_{el} - Z_{ol} = 2\sqrt{2}Z_m Z_s / (Z_{er} - Z_{or}) \tag{3.7}$$

It is apparent from (3.7) that for a given value of Z_m and Z_s, any attempt to reduce the difference $Z_{er} - Z_{or}$ results into corresponding increase in $Z_{el} - Z_{ol}$.

In a special case, when:

$$Z_m = \sqrt{2}Z_s, \text{and } R = 2Z_s \tag{3.8}$$

are chosen, then the design equations for the input and output coupled lines are the same:

$$Z_{el} - Z_{ol} = Z_{er} - Z_{or} = 2Z_s \ . \tag{3.9}$$

3.3 Simulation And Discussion

The general design equations have been developed in the previous section; here they are used to assess the capabilities of the proposed WPD. To that end, we begin with the special case mentioned in (3.8)-(3.9). If Z_s =50Ω, the difference between the even-odd-mode impedances are required to be 100Ω. The simulated S-parameters and phase difference of a design at f_0=2GHz are depicted in Fig. 3.2 for different value of $Z_{ol} = Z_{or} = Z_o$. It is apparent from these simulation results that as the value of Z_o is increased, the corresponding bandwidth of return loss (S_{11}) and that of the transmissions (S_{21}, S_{31}) shrinks. Specifically, the bandwidth for 10dB return loss is 98% for Z_o=20Ω, whereas it shrinks to 70% for Z_o=50Ω. Similar trend is also observed for 14dB return loss (VSWR=1.5). In Fig. 3.2(e) and others, 'iso-con' represents the isolation of conventional WPD. For isolation (S_{23}) bandwidth, if 10dB isolation criteria is adopted then the bandwidth is higher than the entire simulated frequency range, that is, more than 150%. However, if 14dB isolation criteria is adopted, then a higher value of Z_o

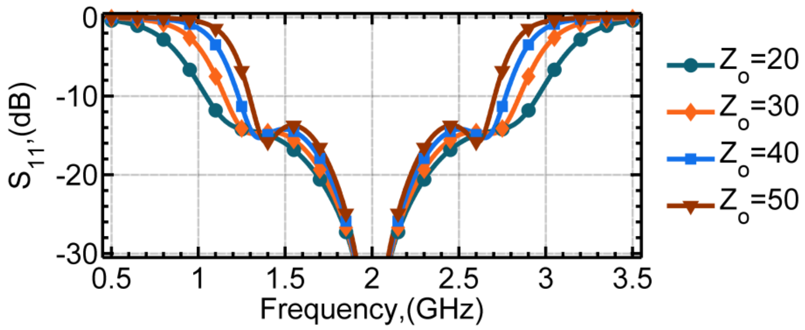
0
-10
-20
-30
S_{11},(dB)
0.5
1
1.5
2
2.5
3
3.5
Frequency,(GHz)
Z_o=20
Z_o=30
Z_o=40
Z_o=50

(a)

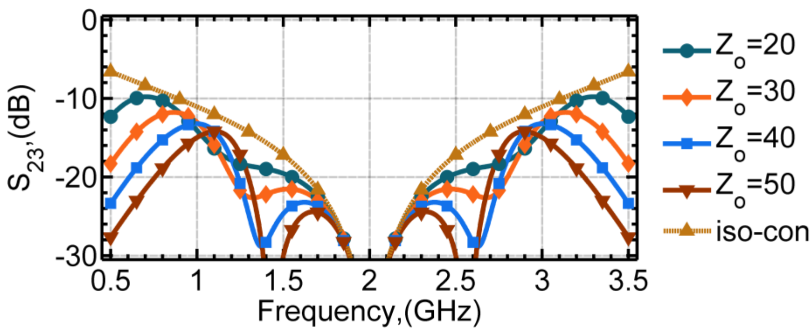
0
-10
-20
-30
S_{23},(dB)
0.5
1
1.5
2
2.5
3
3.5
Frequency,(GHz)
Z_o=20
Z_o=30
Z_o=40
Z_o=50
iso-con

(b)

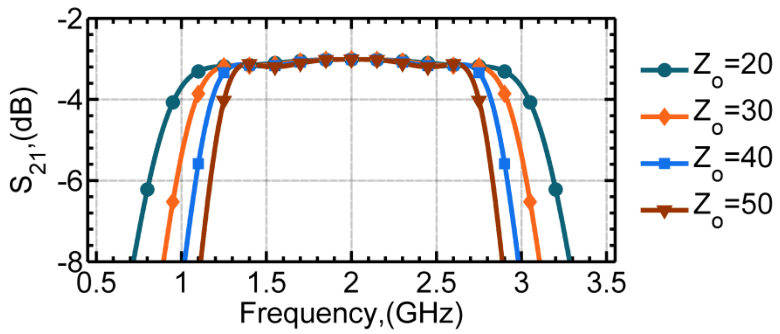
-2
-4
-6
-8
S_{21},(dB)
0.5
1
1.5
2
2.5
3
3.5
Frequency,(GHz)
Z_o=20
Z_o=30
Z_o=40
Z_o=50

(c)

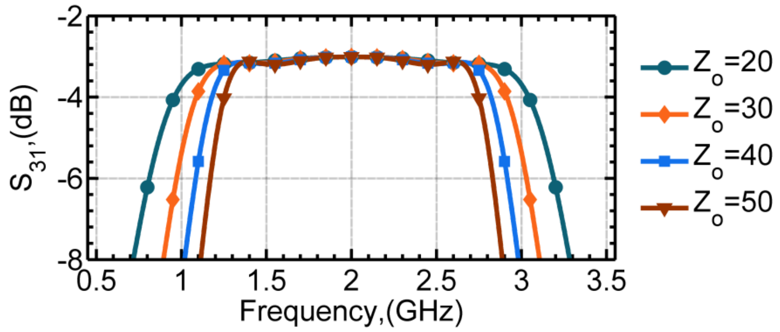
-2
-4
-6
-8
S_{31},(dB)
0.5
1
1.5
2
2.5
3
3.5
Frequency,(GHz)
Z_o=20
Z_o=30
Z_o=40
Z_o=50

(d)

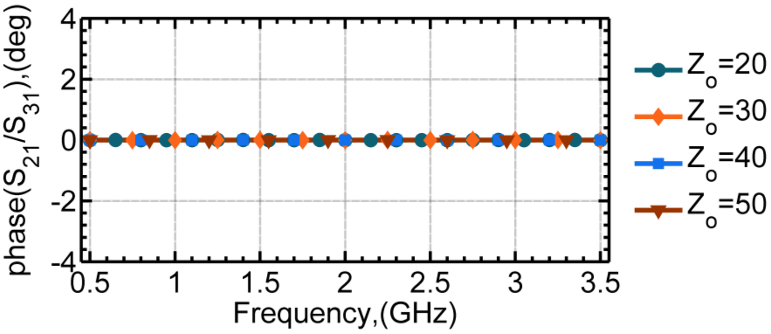

(e)

Fig. 3.2. Simulated S-parameters and phase difference of the proposed WPD for different values of Z_o. 'iso-con': conventional WPD isolation.

produces higher bandwidth−a scenario conflicting with 14dB return loss criteria. Moreover, the fully symmetric structure causes the phase difference between outputs to remain zero. Consequently, for the sake of brevity, the phase difference will not be shown any further.

If the differences between even and odd-mode impedances are maintained at $2Z_s$, it is also possible to design with distinct values of Z_{ol} and Z_{or}. For instance, Fig. 3.3 shows the simulated results for designs with Z_{ol} = 30Ω, Z_{or} = 20Ω (Fig. 3.3(a)) and Z_{ol} = 40Ω, Z_{or} = 20Ω (Fig. 3.3(b)). It is again apparent that the proposed design is preferred, especially, if a higher isolation criteria is set. Specifically, in Fig. 3.3(a), the 20dB isolation bandwidth of conventional design is only 30%, whereas it is 80% for the proposed design.

Another important observation from Fig. 3.3(b) is that it seems possible to obtain perfect matching at two other points symmetrically located about f_0, which in fact is the reason of widening of bandwidth, but we will not pursue that point further since we see that the isolation bandwidth also reduces slightly in that case. In the next design examples, we change the value of Z_m from $\sqrt{2}Z_s$ (70.7Ω) to 60Ω and 80Ω for two designs. The corresponding value of R = 84.85Ω and 113.14Ω, and therefore, $Z_{er}-Z_{or}$= $Z_{el}-Z_{ol}$=92.11Ω and 106.37Ω, respectively. The simulated S-parameters are shown in Fig. 3.4. It is apparent that depending upon the different isolation criteria, one value of Z_m may be preferred over the other. But, higher Z_m requires a higher difference between even and odd-mode impedances, which may pose difficulty during implementation, and may require, for example, a suspended microstrip technology [39].

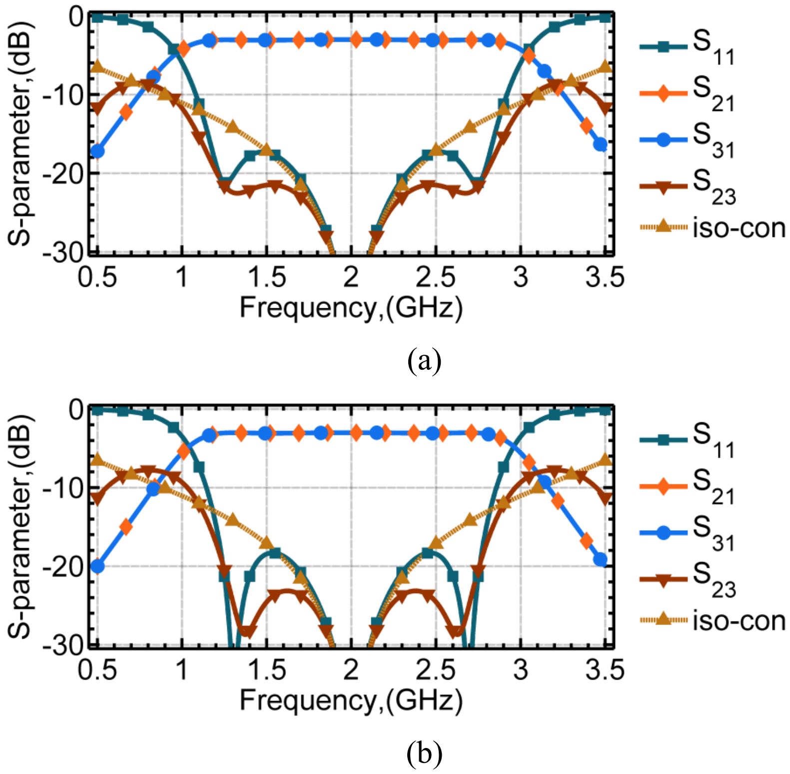

Fig. 3.3. Simulated S-parameters for design with (a) Z_{ol}=30Ω, Z_{or}=20Ω and (b) Z_{ol}=40Ω, Z_{or}=20Ω.

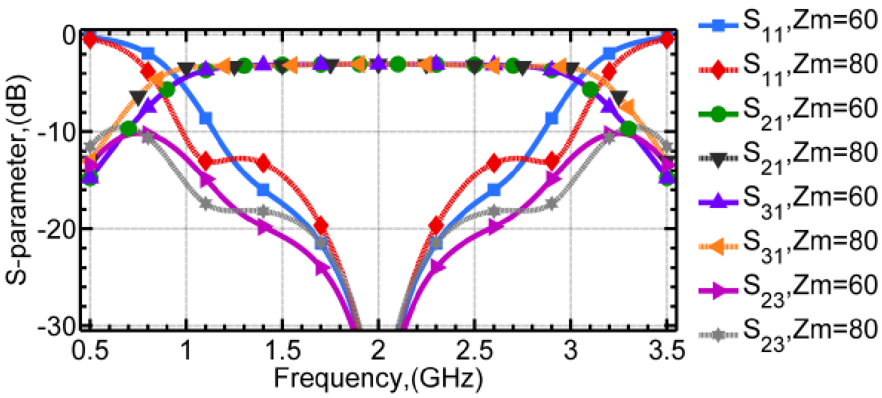

Fig. 3.4. Simulated S-parameters for designs with (a) Z_m=60Ω and (b) Z_m=80Ω. Z_{ol} =Z_{or} =20Ω in both the cases.

3.4 Prototype and measurement

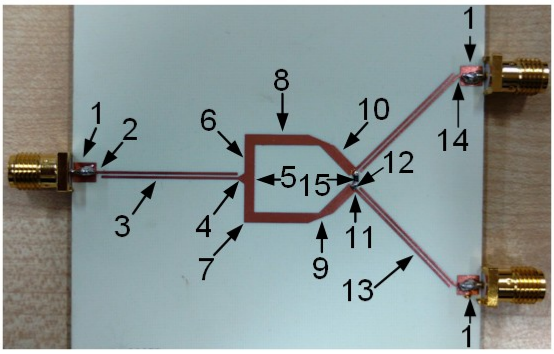

Fig. 3.5. The fabricated prototype. Details of each element in Table 4.1.

TABLE 4.1 DESIGN PARAMETERS OF THE PROTOTYPE(DIMENSIONS: MILS)

#	component	#	component
1	MLIN: W=129, L=150	8	MLIN: W=69, L=350
2	MLIN: W=22, L=30	9	MSABND: W=69, Angle=45, M=0.5
3	MCLIN: W=20, S=8, L=880	10	MLIN: W=69, L=200
4	MTAPER: w1=20, w2=69, l=40	11	MTEE:w1=69, w2=35,w3=18
5	MTEE:w1=w2=w3=69	12	MCURVE: W=35, Angle=45, Radius=35
6	MLIN: W=69, L=185	13	MCLIN: W=18, S=8, L=880
7	Mcorn: w=69	14	MCURVE: W=18, Angle=45, Radius=30
15	Isolation resistor : SMD, Part# CRCW0603100RFKTA (Vishay-Dale)		

A prototype operating at f_0= 2GHz is designed for validation according to (3.8)-(3.9) and with Z_{ol} =Z_{or} =Z_o=50Ω, and implemented on RO4350B substrate (ϵ_r =3.66, height=1.5mm, copper=35μm). To help during layout, some small traces of metals are added, and the final design is optimized to take their and junction discontinuities effects into account. The prototype is shown in Fig. 3.5 along with the details of each element

TABLE 4.2 COMPARISON WITH SOME RECENT DESIGNS

Ref.	Technique	BW(%)	Lumped Elements	DC isolation	Pattern
[36]	Microstrip-to-slotline transition	10dB: 100	2	No	Top+ Bottom
[35]	Complex isolation	20dB: 68 19dB: 75	5	No	Top
This Work	Port-matching	15dB: 65 (EM) 15dB: 62 (Meas)	1	Yes	Top

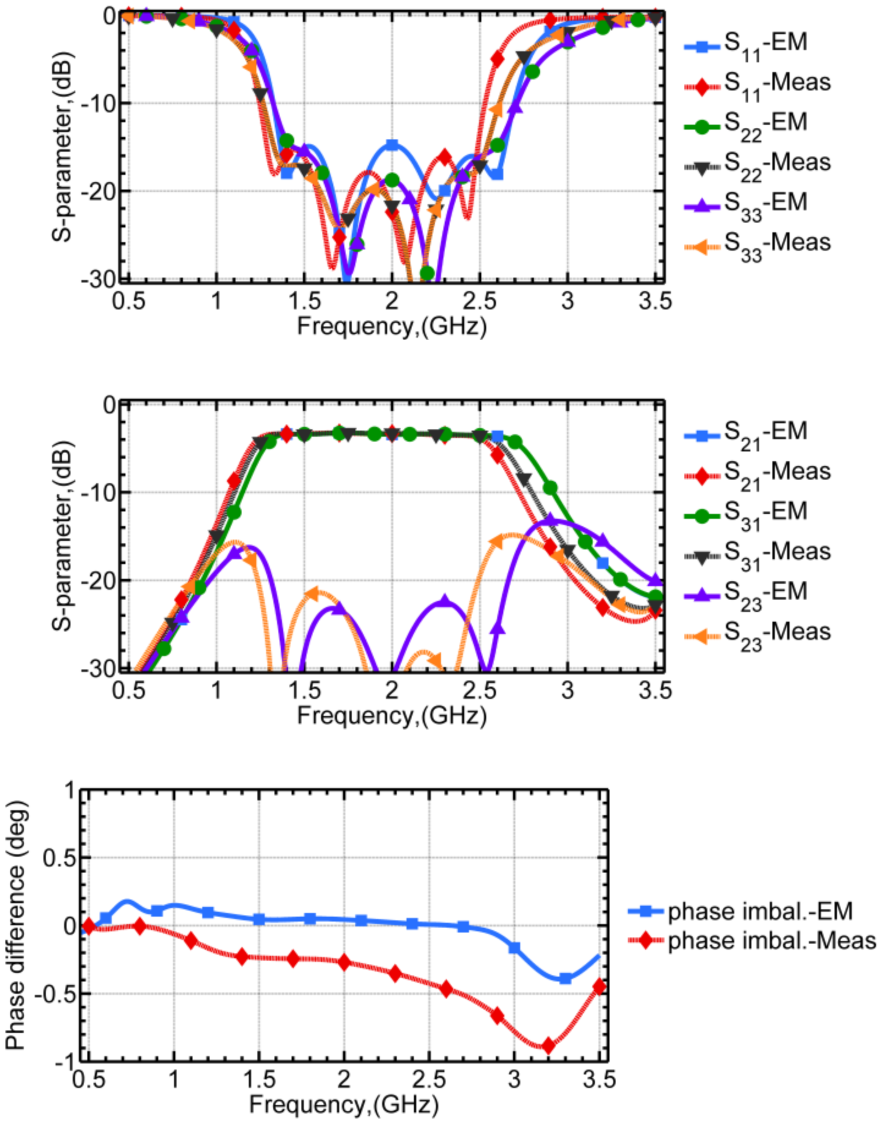

Fig. 3.6. EM simulated and measured S-parameters of the prototype: reflections (top), transmission and isolation (middle), and phase imbalance (bottom).

in Table 4.1. The EM simulated and measurement results are shown in Fig. 3.6, which exhibit good isolation and return loss. While amplitude imbalance within the useful bandwidth (15dB reference/1.25GHz-2.5GHz) is less than 0.2dB, the phase imbalance of around 0.5º is much more than predicted by EM simulation despite a fully symmetrical structure. This is possibly due to fabrication tolerances and due to the non-ideal nature of the isolation resistor. A comparison with current state-of-the-art in Table 4.2 shows promising features of the proposed design. While other designs needs patterning on both side of the PCB or requires more number of lumped elements, the proposed WPD is simple to design and manufacture, provides nice bandwidth, and perfect DC isolation. Lastly, as compared to techniques such as [35], the size of the proposed WPD is obviously larger since it is based on utilization of addition distributed element matching networks at each port. yet, the proposed technique may have lesser area requirement than the techniques [36] using multi-section transmission lines.

3.5 Conclusion

In this chapter, a closed-form design of a DC isolated wideband WPD was presented. The features of the proposed design were explored extensively using simulation carried out using Keysight ADS. The EM simulated and measurement results matches well and thus validates the theory.

Conclusion

There have always been huge interests in the design of wideband RF/microwave components and power dividers are no exception. The Wilkinson power divider (WPD), invented in 1960, is workhorse of today's industry. It has completely matched output ports with sufficiently high isolation between them. This device is also potentially lossless provided that no reflected power from output ports enters into it. This divider has wide applications in microwave system and devices but it has a narrow bandwidth. Several attempts have been reported in the literature to enhance the bandwidth of WPDs, and utilization of multi-section/tapered line matching network is very common among them. The techniques which propose to modify the isolation network employing reactive lumped elements have gained momentum in the past few years.

The objective of this thesis was to pursue some uncommon techniques to tackle this problem. To that end, a scheme to get best out of the advantages that WPD and GPD offer was discussed in Chapter 2. Specifically, a clear design methodology to for Power divider as a combination of GPD and WPD employing only one isolation resistor was discussed. It is found that considering 15dB return-loss reference, the bandwidth is 72% for the proposed design whereas it is only 36% for earlier reported design.

By employing matching network at each port of conventional Wilkinson divider core structure, a novel WPD with fairly good performance was described in Chapter 3. Specifically, parallel coupled lines were used at each port to facilitate a wideband matching. Due to the use of these coupled line structure, a DC isolated WPD is obtained which can be potentially be used in balanced amplifiers with having requirement of coupling capacitors. A prototype was fabricated to validate the proposed theory. The EM simulated results matches quite well with the measured results and the measured isolation bandwidth is 62% considering 15dB reference.

Bibliography

1. D. M. Pozar, *Microwave Engineering*, 3rd ed., New Delhi: J. Wiley & Sons, 2010.
2. Microwave power dividers and couplers tutorial: overview and definition of terms (online), Accessed: July 04, 2016, URL: https://www.markimicrowave.com/Assets/appnotes/microwave_power_dividers_and_couplers_primer.pdf
3. www.microwaves101.com
4. R. Gómez-García, R. Loeches-Sanchez, D. Psychogiou, and D. Peroulis, "Single/multi-band Wilkinson-type power dividers with embedded transversal filtering sections and application to channelized filters," *IEEE Trans. Circuits Syst. I, Reg. Papers*, vol. 62, no. 6, pp. 1518–1527, Jun. 2015.
5. X. Wang, I. Sakagami, K. Takahashi, and S. Okamura, "A generalized dual-band Wilkinson power divider with parallel L, C, and R components," *IEEE Trans. Microw. Theory Techn.*, vol. 60, no. 4, pp. 952–964, Apr. 2012.
6. N. Gao, G. Wu, and Q. Tang, "Design of a novel compact dual-band Wilkinson power divider with wide frequency ratio," *IEEE Microw. Wireless Compon. Lett.*, vol. 24, no. 2, pp. 81–83, Feb. 2014.
7. A. Genc and R. Baktur, "Dual- and triple-band Wilkinson power dividers based on composite right- and left-handed transmission lines," *IEEE Trans. Compon., Packag., Manuf. Technol.*, vol. 1, no. 3, pp. 327–334, Mar. 2011.
8. K.-K. M. Cheng and F.-L. Wong, "A new Wilkinson power divider design for dual band application," *IEEE Microw. Wireless Compon. Lett.*, vol. 17, no. 9, pp. 664–666, Sep. 2007.
9. Y. Shin, B. Lee, and M. -J. Park, "Dual-band Wilkinson power divider with shifted output ports," *IEEE Microw. Wireless Compon. Lett.*, vol. 18, no. 7, pp. 443–445, Jul. 2008.
10. G. Wu, L. Yang, Y. Zhou and Q. Xu, "Wilkinson power divider design for dual-band applications," *IET Electron. Lett.*, vol. 50, no. 1 4, pp. 1003–1005, July 2014.

11. Y. -C. Liu, W. -H. Chen, X. Li and Z. -H. Feng, "Compact design of dual-band power divider with coupled-line shunt elements," *IET Electron. Lett.*, vol. 47, no. 4, pp.262–263, Feb. 2011.
12. S. Cohn, "A class of broadband three-port TEM-mode hybrids," *IEEE Trans. Microw. Theory Tech.*, vol. MTT-19, no. 2, pp. 110–116, Feb. 1968.
13. R. Ekinge, "A new method of synthesizing matched broad-band TEM mode three-ports," *IEEE Trans. Microw. Theory Tech*., vol. MTT-19, no. 1, pp. 81–88, Jan. 1971.
14. H. Oraizi and A.-R. Sharifi, "Design and optimization of broadband asymmetrical multisection Wilkinson power divider," *IEEE Trans. Microw. Theory Tech*., vol. 54, no. 5, pp. 2220–2231, May 2006.
15. H. Oraizi and A. R. Sharifi, "Optimum design of asymmetrical multisection two-way power dividers with arbitrary power division and impedance matching," *IEEE Trans. Microw. Theory Tech*., vol. 59, no. 6, pp. 1478-1490, Jun 2011.
16. N. Ehsan, K. Vanhille, S. Rondineau, E. Cullens, and Z. Popovic, "Broadband micro-coaxial Wilkinson dividers," *IEEE Trans. Microw. Theory Tech*., vol. 57, no. 11, pp. 2783–2789, Nov. 2009.
17. C. T. Chiang and B.-K. Chaung, "Ultra wideband power divider using tapered line," *Progress In Electromagnetics Res*, vol. 106, pp. 61–73, 2010.
18. S. W. Wong and L. Zhu, "Ultra-wideband power dividers with good isolation and improved sharp roll-off skirt," *IET Microwaves, Antennas & Propagation*, vol. 3, no. 8, pp. 1157-1163, December 2009.
19. J. C. Kao, Z. M. Tsai, K. Y. Lin and H. Wang, "A modified Wilkinson power divider with isolation bandwidth improvement," *IEEE Trans. Microw. Theory Tech*., vol. 60, no. 9, pp. 2768-2780, Sept. 2012.
20. R. Mirzavand, M. M. Honari, A. Abdipour and G. Moradi, "Compact microstrip Wilkinson power dividers with harmonic suppression and arbitrary power division ratios," *IEEE Trans. Microw. Theory Tech*., vol. 61, no. 1, pp. 61-68, Jan. 2013.
21. I. -H. Lin, M. D. Vincentis, C. Caloz, and T. Itoh, "Arbitrary dual-band components using composite right/left-handed transmission lines," *IEEE Trans. Microwave Theory Tech.*, vol. 52, pp. 1142–1148, Apr. 2004.

22. W. -H. Chen, Y. -C. Liu, X. Li, Z. -H. Feng, and F. M. Ghannouchi, "Design of reduced-size unequal power divider for dual-band operation with coupled lines," *IET Electron. Lett.*, vol. 47, no. 1, pp.59–60, Jan. 2011.
23. X. Wang, I. Sakagami, A. Mase and M. Ichimura, "Wilkinson power divider with complex isolation component and its miniaturization," *IEEE Trans. Microw. Theory Tech*., vol. 62, no. 3, pp. 422-430, March 2014.
24. W. M. Chau, K. W. Hsu and W. H. Tu, "Filter-based Wilkinson power divider," *IEEE Microwave and Wireless Components Letters*, vol. 24, no. 4, pp. 239-241, April 2014.
25. H. R. Ahn and S. Nam, “3-dB power dividers with equal complex termination impedances and design methods for controlling isolation circuits,” *IEEE Trans. Microw. Theory Tech.*, vol. 61, no. 11, pp. 3872–3883, Nov. 2013.
26. X. Wang, K.L. Wu, and W.Y. Yin, "A compact Gysel power divider with unequal power-dividing ratio using one resistor," *IEEE Trans. Microw. Theory Techn.*, vol. 62, No. 7, pp. 1480–1486, July 2014.
27. Y. Kim, S.-H. Kim, and Y.-C. Yoon, " An unequal Gysel power divider based on circuit transformation," *Wiley Microw. Opt. Technol. Lett.*, vol. 57, No. 7, pp. 1529–1531, July 2015.
28. J. Guan, L. Zhang, Z. Sun, Y. Leng, and Y. Peng, "Designing power divider by combining Wilkinson and Gysel structure," *IET Electron. Lett.*, vol.48, no.13, pp. 769-770, June 2012.
29. R. Zaker, A. Abdipour, and R. Mirzavand, "Closed-form design of Gysel power divider with only one isolation resistor," *IEEE Microw. Wireless Compon. Lett.*, vol.24, No. 8, pp.527–529, Aug. 2014.
30. M. A. Maktoomi, M.S. Hashmi, and F. M. Ghannouchi, “A T-Section Dual-Band Matching Network For Frequency-Dependent Complex Loads Incorporating Coupled Line With Dc-Block Property Suitable For Dual-Band Transistor Amplifiers,” *Prog. Electromagn. Res.* C (*PIER C*), vol. 54, pp.75-84, 2014.
31. M. Hayati, S.-A. Malakooti, and A. Abdipour, "A novel design of triple-band Gysel power divider," *IEEE Trans. Microw. Theory Techn.*, vol.61, no.10, pp.3558-3567, Oct. 2013.

32. M. A. Maktoomi and M. S. Hashmi, "A novel power divider structure using the gysel and wilkinson power dividers with only one grounded resistor," *2015 IEEE MTT-S International Microwave and RF Conference (IMaRC)*, Hyderabad, pp. 227-229, 2015.
33. S. -F. Chao and Y. -R. Li, "Miniature filtering power divider with increased isolation bandwidth," *IET Elect. Lett.,* vol. 50, no. 8, pp. 608–610, Apr. 2014.
34. H. R. Ahn, B. Kim, and S. Nam, "Compact UHF 3 dB MCCT power dividers," *IEEE Microw. Wireless Compon. Lett.*, vol. 24, no. 7, pp. 445–447, Jul. 2014.
35. V. Tas and A. Atalar, "An optimized isolation network for the Wilkinson divider," *IEEE Trans. Microw. Theory Tech.,* vol. 62, no. 12, pp. 3393–3402, Dec. 2014.
36. U. T. Ahmed and A. M. Abbosh, "Modified Wilkinson power divider using coupled microstrip lines and shunt open-ended stubs," *IET Elect. Lett.,* vol. 51, no. 11, pp. 838–839, May 2015.
37. Y. Wu, Y. Liu, Y. Zhang, J. Gao, and H. Zhou, "A dual-band unequal Wilkinson power divider without reactive components," *IEEE Trans. Microw. Theory Tech.*, vol. 57, no. 1, pp. 216–222, Jan. 2009.
38. Q.-X. Chu, F. Lin, Z. Lin, and Z. Gong, "Novel design method of triband power divider," *IEEE Trans. Microw. Theory Techn.*, vol. 59, no.9, pp. 2221–2226, Sep. 2011.
39. W. A. Arriola, J. Y. Lee, and I. S. Kim, "Wideband 3 dB branch line coupler based on λ/4 open circuited coupled lines," *IEEE Microw. Wireless Compon. Lett.*, vol. 21, no. 9, pp. 486–488, Sept. 2011.
40. M. A. Maktoomi, M. S. Hashmi and F. M. Ghannouchi, "Theory and design of a novel wide-band dc isolated Wilkinson power divider," *IEEE Microw. Wireless Compon. Lett.*, 2016 (Accepted for publication).

Biography and Curriculum Vitae

Mohammad A. Maktoomi was born in Sasauli− a remote village in India in 1985. He received the B.Tech. degree in electronics engineering from Aligarh Muslim University (AMU), Aligarh, India, in 2009, and is currently working toward the Ph.D. degree in electronics and communication engineering at the Indraprastha Institute of Information Technology Delhi, New Delhi, India.

He has served with the Hindustan College of Science and Technology, Mathura, India, as an Assistant Professor, and AMU as a Guest Faculty member. From October 2015 to April 2016, he was with the iRadio Laboratory, University of Calgary, Canada, as a Visiting Ph.D. Student. He has published in many international conferences and reputed journals. He is a regular reviewer for many esteemed journals, and has been invited to many workshops to present tutorials. His current research interests include multiband RF/microwave circuits and current-mode analog circuits.

Mr. Maktoomi was a recipient of the Best Student Paper Award at the IEEE IMPACT, India, in 2013, in the RF/microwave category. He was the winner in the Keysight IEEE MTT-S Student Design Contest on Microstrip Filter Design.

When he is not doing research, he enjoys making tutorials.

Mohammad A. Maktoomi, PhD Candidate, IIIT Delhi, India

CONTACT INFORMATION

University:
PhD Lab 3A (old), IIIT Delhi
Okhla Industrial Estate, Phase III
Near Govindpuri Metro
New Delhi 110020
India
E-mail: ayatullahm@iiitd.ac.in

Home:
E-86 (2^{nd} Floor)
Shaheen Bagh
Jamia Nagar, Okhla
New Delhi 110025
India
Voice: (+91) 9990730806

NATIONALITY

Indian

RESEARCH INTERESTS

Multi-Band/Wideband RF/Microwave Active and Passive Components, RF Power Amplifier Design, RF Energy Harvesting, Wireless Power Transfer, Analog Electronics

EDUCATION

Indraprastha Institute of Information Technology Delhi (IIITD), New Delhi, India

Ph.D. Candidate in RF/Microwave Engineering Since February 2013
(Thesis submitted: July 2016; Expected Graduation: August 2016)

- Dissertation Topic: "Analytical Formulations for Systematic Design of Dual-/Tri-Frequency Impedance Transformation Networks Required in Software-Defined Radios (SDRs) and Energy Harvesting Applications."
- Advisor: Dr. Mohammad S. Hashmi, Assistant Professor, IIITD

Indraprastha Institute of Information Technology Delhi (IIITD), New Delhi, India

Master of Technology (M.Tech.), Electronics and Communication Engineering,
(Thesis submitted: June 2016; Expected Graduation: July 2016)

- Dissertation Topic: "High Bandwidth Planar Power Divider."
- Advisor: Dr. Mohammad S. Hashmi, Assistant Professor, IIITD

Aligarh Muslim University, Aligarh, U.P., India

Bachelor of Technology (B.Tech.), Electronics Engineering, July 2005 - May 2009

HONORS AND AWARDS

- IIIT Delhi Overseas Research Fellowship
- **Winner** of the Keysight IEEE MTT-S International Microwave and RF Conference (IMaRC) Filter Design Competition 2015
- **Best paper award** in the technical session of microwave at the IEEE International Conference on Multimedia, Signal Processing and Communication Technologies (IMPACT) 2013

RESEARCH INTERNSHIP

iRadio Lab, University of Calgary, Alberta, Canada

Visiting PhD Student **October 2015 - April 2016**

Worked with Prof. Fadhel M. Ghannouchi on the design of Multi-Band RF Active and Passive Components

ACADEMIC EXPERIENCE

Indraprastha Institute of Information Technology Delhi (IIITD), New Delhi, India

Teaching Assistant **August 2013 - September 2015**

Duties at various times have included office hours for undergraduate and graduate student projects and leading weekly tutorial and lab exercises in Analog Circuit Design and Electromagnetism

Aligarh Muslim University, Aligarh, U.P., India

Guest Faculty **August 2011 - June 2012**

Taught undergraduate level courses: Basic Electronics, Digital Electronics, SPICE Simulation and associated labs.

Hindustan College of Science and Technology, Mathura, U.P., India

Assistant Professor **July 2009 - May 2011**

Taught undergraduate level courses: Analog Integrated Electronics, Semiconductor Devices, SPICE Simulation and associated labs.

Research and Publications

Under Review Articles

M. A. Maktoomi, M. Akbarpour, M. S. Hashmi, and F. M. Ghannouchi, "On the dual-frequency impedance/admittance characteristic of multi-section commensurate transmission-line," *IEEE Transactions on Circuits and Systems II: Express Briefs.*

M. A. Maktoomi, M. S. Hashmi, and F. M. Ghannouchi, "A dual-band port extended branch-line coupler and mitigation of the band-ratio and power division limitations," *IEEE Transactions on Components, Packaging and Manufacturing Technology.*

M. A. Maktoomi, A. P. Yadav, M. S. Hashmi, and F. M. Ghannouchi, "Performance enhancement of dual-frequency impedance matching networks using dual-frequency property of two-section transmission-line terminated into a real impedance," *IET Microwaves, Antennas and Propagation.*

M. A. Maktoomi and M. S. Hashmi, "A novel enhanced band-ratio dual-band Wilkinson power divider with option of partial port extension," *IEEE Transactions on Microwave Theory and Techniques.*

M. A. Maktoomi, M. H. Maktoomi, Ajay P. Yadav, M. S. Hashmi, and F. M. Ghannouchi, "Dual-frequency admittance property of two sections transmission-line and application," *2016 IEEE* 59^{th} *Midwest Symposium on Circuits and Systems (MWSCAS'2016).*

R. Gupta, **M. A. Maktoomi**, and M. S. Hashmi, "A new high frequency balun with simplified impedance matching technique," *2016 Asia-Pacific Microwave Conference (APMC'2016).*

Peer-Reviewed Journal Articles

M. A. Maktoomi, M. S. Hashmi, and F. M. Ghannouchi, "Theory and design of a novel wideband DC isolated Wilkinson power divider," *IEEE Microwave Wireless Components Letters*, 2016 (Accepted)

M. A. Maktoomi, M. Akbarpour, M. S. Hashmi, and F. M. Ghannouchi, "A theorem for multi-frequency DC-feed network design," *IEEE Microwave Wireless Components Letters*, 2016 (Accepted)

M. A. Maktoomi, M. S. Hashmi, and F. M. Ghannouchi, "Improving load range of dual-band impedance matching networks using novel load-healing concept," *IEEE Transactions on Circuits and Systems II: Express Briefs*, 2016 (Accepted).

M. A. Maktoomi, M. S. Hashmi, and F. M. Ghannouchi, "Systematic design technique for dual-band branch-line coupler using T- and Pi-networks and a novel wide band-ratio crossover," *IEEE Transactions on Components, Packaging and Manufacturing Technology*, vol. 6, No. 5, pp. 784-795, Apr. 2016.

M. A. Maktoomi, M. S. Hashmi, A. P. Yadav, and V. Kumar, "A generic tri-band matching network," *IEEE Microwave Wireless Components Letters*, vol. 26, No. 5, pp. 316-318, Apr. 2016.

M. A. Maktoomi, M. S. Hashmi, and V. Panwar, "A dual-frequency matching network for FDCLs using dual-band $\lambda/4$-lines," *Progress In Electromagnetics Research L*, vol. 52, pp. 23-30, 2015.

M. A. Maktoomi and M. S. Hashmi, "A coupled-line based l-section DC-isolated dual-band real to real impedance transformer and its application to a dual-band T-junction power divider," *Progress In Electromagnetics Research C*, vol. 55, pp. 95-104, 2014.

M. A. Maktoomi, M. S. Hashmi, and F. M. Ghannouchi, "A T-section dual-band matching network for frequency-dependent complex loads incorporating coupled line with DC-block property suitable for dual-band transistor amplifiers," *Progress In Electromagnetics Research C*, vol. 54, pp. 75-84, 2014.

Conference Proceedings

S. Kumar, S. Kaushik, R. Gupta, **M. A. Maktoomi**, and M. S. Hashmi, "A new L-shaped phase inverter design utilizing a loaded transmission line," in IEEE MTT-S IWS 2016, Shanghai, China, March 2016. (Accepted)

M. A. Maktoomi and M. S. Hashmi, "A CAD assisted design methodology for wideband arbitrary power division coupler implemented in microstrip technology," in IEEE 22^{nd} NCC 2016, IIT Guwahati, India, March 2016. (Accepted)

M. A. Maktoomi and M. S. Hashmi, "A novel power divider structure using the Gysel and Wilkinson power dividers with only one grounded resistor," in IEEE MTT-S IMaRC'2015, Hyderabad, India, December 2015. (Accepted)

M. A. Maktoomi, R. Gupta, M. S. Hashmi, "A dual-band impedance transformer for frequency-dependent complex loads incorporating an L-type network," in 2015 Asia-Pacific Microwave Conference (APMC'2015), Nanjing, China, December 2015. (Accepted)

M. A. Maktoomi, V. Panwar, M. S. Hashmi, and F. M. Ghannouchi, "A dual-band matching network for frequency-dependent complex loads suitable for dual-band RF amplifiers," in IEEE MTT-S IMaRC'2014, Bangalore, India, December 2014.

Z. N. Zafar, **M. A. Maktoomi**, and M. S. Hashmi, "New adjustable square/triangular- wave generators using CCII/CCCII and OTA," IEEE ICM, Qatar, December 2014.

P. Aggarwal, V. Mittal, **M. A. Maktoomi**, and M. S. Hashmi, "A CMOS digitally controlled floating positive resistor using translinear cells," in IEEE RAECS, Chandigarh, India, March 2014.

A. Jain, **M. A. Maktoomi**, and M. S. Hashmi, "A new circuit to measure resistance variation suitable for strain gauge," in IEEE SPIN, Noida, India, February 2014.

M. A. Maktoomi, A. M. Zaidi, and M. S. Hashmi, "A dual-band Bagley power divider using modified -Network," in IEEE IMPACT, Aligarh, India, November 2013.

M. A. Maktoomi, M. A. Siddiqi, S. A. Rahman, and R. K. Mishra, "An interface circuit for measuring small as well as large resistance changes," in IEEE ICATE, Mumbai, India, January 2013.

M. A. Maktoomi, M. Singh, and M. A. Siddiqi, "High bandwidth circuits for the measurement of small resistance changes," in IEEE ICPCES, Allahabad, India, December, 2012.

M. A. Maktoomi, M. A. Siddiqi, and M. P. Pyari, "FVF based CDTA and its application," in IEEE ICCICT, Mumbai, India, October 2012.

M. A. Maktoomi, R. K. Mishra, M. A. Siddiqi, and M. P. Pyari, "CDTA based logarithmic amplifier," in IEEE ISPCC, Solan, India, March 2012.

MEMBERSHIP

IEEE MTT-S Graduate Student Member

RELEVANT SKILLS

- EDA Packages: Keysight ADS, HFSS, SPICE, MATLAB/octave, gnuplot.
- Language: C.
- Applications: Xcircuit, LaTeX, spreadsheet, and presentation software.
- Operating Systems: Unix/Linux, Windows.
- Speaking and Writing level skills in English, Hindi and Urdu languages

REFERENCES

Dr. Mohammad S. Hashmi, Assistant Professor, Electronics and Communication Engineering, IIITD, Okhla Phase-3, New Delhi -110020, India, mshashmi@iiitd.ac.in

Dr. Fadhel M. Ghannouchi, Professor, Department of Electrical and Computer Engineering, University of Calgary, Alberta, Canada, fghannou@ucalgary.ca

Dr. S. A. Rahman, Professor, Electronics Engineering, Aligarh Muslim University, Aligarh-202002, U.P., India, atiqamu@gmail.com

Dr. Ekram Khan, Professor, Electronics Engineering, Aligarh Muslim University, Aligarh-202002, U.P., India, ekhan67@gmail.com